CHEMISTRY
A EUROPEAN JOURNAL

DOI: 10.1002/chem.200902377

A Nucleic Acid Dependent Chemical Photocatalysis in Live Human Cells

Dumitru Arian,[a] Emiliano Cló,[b] Kurt V. Gothelf,[b] and Andriy Mokhir*[a]

Abstract: Only two nucleic acid directed chemical reactions that are compatible with live cells have been reported to date. Neither of these processes generate toxic species from nontoxic starting materials. Reactions of the latter type could be applied as gene-specific drugs, for example, in the treatment of cancer. We report here the first example of a chemical reaction that generates a cytotoxic drug from a nontoxic prodrug in the presence of a specific endogeneous ribonucleic acid in live mammalian cells. In this case, the prodrug is triplet oxygen and the drug is singlet oxygen. The key component of this reaction is an inert molecule (InP–2′-OMe-RNA/Q–2′-OMe-RNA; P: photosensitizer; Q: quencher), which becomes an active photosensitizer (InP–2′-OMe-RNA) in the presence of single-stranded nucleic acid targets. Upon irradiation with red light, the photosensitizer produces over 6000 equivalents of toxic singlet oxygen per nucleic acid target. This reaction is highly sequence specific. To detect the generation of singlet oxygen in live cells, we prepared a membrane-permeable and water-soluble fluorescent scavenger, a derivative of 2,5-diphenylisobenzofurane. The scavenger decomposes upon reaction with singlet oxygen and this is manifested in a decrease in the fluorescence intensity. This effect can be conveniently monitored by flow cytometry.

Keywords: live cells · nucleic acids · photocatalysis · photosensitizers · singlet oxygen

Introduction

Several types of nucleic acid controlled chemical reactions have been reported, including templated ligation, cleavage, group transfer, and a variety of photoinduced processes.[1] A majority of them were designed for in vitro applications,[1–3] and only two such reactions were found to be compatible with living cells. In particular, Kool and co-workers have shown that ligation between 3′-nucleophilic phosphorothioate and 5′-electrophilic probes is triggered by endogeneous RNAs, both in bacteria and in mammalian cells.[4] Three research groups have independently reported that the Staudinger reaction is accelerated by RNAs in human embryonic kidney 293 (HEK293) and HL-60 cells.[5] Although these chemical processes are highly sequence specific, they exhibit relatively low maximal turnover numbers (TON_{max}) of 7–92. This limits their applicability to the detection of abundant RNAs.

Nucleic acid dependent reactions that are compatible with live cells are especially interesting, because they can be applied not only for monitoring endogeneous RNAs in situ but also for the RNA-dependent release of cytotoxic drugs (gene-encoded prodrugs).[1] Such drugs can, for example, selectively kill cancer cells, which are usually genetically different from normal cells. The latter possibility has not been demonstrated yet. In general, the adaptation of chemical reactions to live-cell conditions is a challenging task,[5,6] because of the poor membrane permeability and toxicity of the reagents and the presence of a rather complex mixture of different compounds in the cell, which may facilitate undesired side reactions. Several nucleic acid directed reactions that convert prodrugs into drugs have been reported to work in vitro.[7] For example, Saito and co-workers and Tanabe, Nishimoto, and co-workers have described the stoichiometric UV-light-induced generation of model drugs. The addition of the specific nucleic acid increases the yields of the products in these reactions by 2- to 7-fold.[7a,b] Gothelf and co-workers have reported a reaction that can generate toxic $^1O_2$ (the drug) from nontoxic $^3O_2$ (the prodrug).[7c] In

[a] D. Arian, Dr. A. Mokhir
Anorganisch-Chemisches Institut
Ruprecht-Karls-Universität Heidelberg
Im Neuenheimer Feld 270, 69120 Heidelberg (Germany)
Fax: (+49) 6221-548439
E-mail: Andriy.Mokhir@urz.uni-heidelberg.de

[b] Dr. E. Cló, Prof. Dr. K. V. Gothelf
Centre for DNA Nanotechnology
Department of Chemistry and iNANO
Aarhus University
Langelandsgade 140, 8000 Århus C (Denmark)

Supporting information for this article is available on the WWW under http://dx.doi.org/10.1002/chem.200902377.

particular, they have prepared a duplex from the (pyropheophorbide-*a*)–oligodeoxyribonucleotide conjugate (**P**–ODN1; **P**: pyropheophorbide-*a* photosensitizer; Figure 1) and the

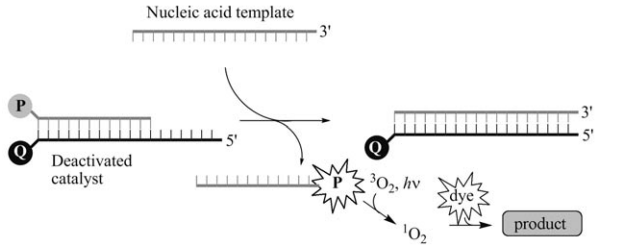

Figure 1. Nucleic acid induced catalytic decomposition of a scavenger (dye). The dye reacts with singlet oxygen to produce a colorless product. "P" on a gray background indicates a deactivated photosensitizer, "P" on a white background (inside the star) indicates the activated photosensitizer, and "Q" in black-colored circles indicates a quencher; all sequences are arbitrary.

complementary **Q**–ODN2 (**Q**: quencher). In this associate, the **P** is fully quenched by the **Q**, whereas in the presence of an analyte nucleic acid, the **P**–ODN1 conjugate is set free and the **P** is reactivated. In the active form, the **P** induces the generation of $^1O_2$ when exposed to light. This effect could be observed only at rather high concentrations of the duplex (5 μM) and in the D_2O buffer,[7c] conditions that are not compatible with live cells. This reaction is not catalytic, because the **P** decomposes quickly in the presence of $^1O_2$.

Herein, we report on two key modifications of the known system: we use a more sensitive method for $^1O_2$ monitoring and substitute the **P** for a more potent and stable photosensitizer. The resulting nucleic acid controlled photocatalyst is active in aqueous buffer, exhibits the highest turnover frequency and number among the known analogous chemical catalysts, and is able to generate toxic $^1O_2$ in the presence of specific nucleic acids in live cells.

Results and Discussion

In^{3+} complexes with **P** and its derivatives are substantially more active photodynamic agents than the parent ligands.[8] One of the reasons for this could be that they are better photosensitizers under physiological conditions. Therefore, we decided to substitute the pyropheophorbide-*a* in **P**–ODN for the In^{3+} complex, In**P**. It has been reported that In**P**–OH, which is required for the synthesis of the ODN conjugates, can be obtained by treatment of **P**–OH with $InCl_3$ in benzene.[8] In our hands, this reaction yielded only traces of the complex. We believe the reason for this is that both reagents, $InCl_3$ and **P**–OH, are almost insoluble in benzene. For an alternative metal-complex formation procedure, we used a soluble allyl ester of pyropheophorbide-*a* (**P**–Oallyl) in place of the **P**–OH. **P**–Oallyl was obtained by acid-catalyzed transesterification of phytyl pheophorbide-*a*, followed by decarboxylation of the resulting allyl pheophorbide-*a* (Scheme 1). The reaction of this compound with $InCl_3$ in benzene furnished In**P**–Oallyl in 62% yield. The allyl group was cleanly removed in the presence of $[Pd(PPh_3)_4]$ to obtain In**P**–OH. The complex was conjugated to different ODN and 2′-OMe-RNA sequences by using solid-phase synthesis.

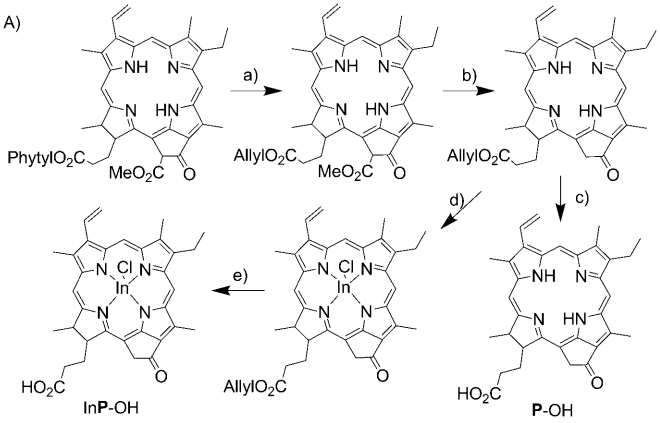

B) 5'→3':

P–ODN1: **P**–CGCACCATAAACCTT
In**P**–ODN1: In**P**–CGCACCATAAACCTT
In**P**–ODN2–**Q**: In**P**–GCGAGCCACCAAACATGATATGCTCGC–BHQ-3
In**P**–2'-OMe-RNA3: In**P**–AUGCUGAUGUUCUAAG
In**P**–2'-OMe-RNA4: In**P**–CAGAUCUUGGUGGUAG
In**P**–2'-OMe-RNA5: In**P**–AUGCUGAUGUUCUAAGCUAC
In**P**–2'-OMe-RNA6: In**P**–CAGAUCUUGGUGGUAGUAGC

Q–ODN7: GGTCTGAAGGTTTATGGTGCG–BHQ-3
Q–2'-OMe-RNA8: GAGUAGCUUAGAACAUCAGCAU–BHQ-3
Q–2'-OMe-RNA9: UUGCUACUACCACCAAGAUCUG–BHQ-3
Q–2'-OMe-RNA10: GGAUUAAUGAGUAGCUUAGAACAUCAGCAU–BHQ-3
Q–2'-OMe-RNA11: UUGAAUAUUUGCUACUACCACCAAGAUCUG–BHQ-3

DNA12: CGCACCATAAACCTTCAGACC
RNA13: CGCACCAUAAACCUUCAGACC
DNA14: CGCACCAAAAACCTTCAGACC
DNA15: AAAGAAAATATCATGTTTGGTGTTTCCTAT
DNA16: AAAGAAAATATCATCTTTGGTGTTTCCTAT

Scheme 1. A) Preparation of photosensitizers **P**–OH and In**P**–OH: a) Allyl-OH, H_2SO_4; b) 2,4,6-collidine, 170 °C; c) $[Pd(PPh_3)_4]$, $(Et_2NH_2)(HCO_3)$; d) $InCl_3$; e) $[Pd(PPh_3)_4]$, $(Et_2NH_2)(HCO_3)$. B: Sequences of the conjugates and nucleic acids used in this study. BHQ-3: black-hole quencher-3.

Next, we developed a fluorescent scavenger (denoted as "dye" in Figure 1) for monitoring the formation of $^1O_2$ in live human cells. $^1O_2$ was previously detected by monitoring its weak phosphorescence at 1270 nm.[7c] Fluorescent probes offer higher $^1O_2$ sensitivity and easier signal detection. Known reagents of this type include trans-1-(2-methoxyvinyl)pyrene (MVP), dansyl-2,2,5,5-tetramethyl-2,5-dihydro-1*H*-pyrrole (DanePy), fluorescein-based compounds such as 9-[2-(3-carboxy-9,10-dimethyl)anthryl]-6-hydroxy-3*H*-xanthen-3-one (DMAX) or 9-[2-(3-carboxy-9,10-diphenyl)anthryl]-6-hydroxy-3*H*-xanthen-3-one (DPAX), 1,3-diphenylisobenzofuran (DPBF), and single-oxygen sensor green (SOSG). They have been used for monitoring $^1O_2$ in vitro. DanePy and SOSG have been applied for the detection of

$^1O_2$ in plant cells and plants.[9] No probe has been demonstrated to be applicable for monitoring $^1O_2$ in mammalian cells. The lifetime of $^1O_2$ in aqueous buffer is very short ($\approx$3.5 μs)[10] and it is further reduced by intracellular quenchers,[10] so we selected DPBF as a lead structure. The reaction of DPBF with $^1O_2$ is very fast and it is only $\approx$40 times slower than the diffusion-limited value, $k_M = 7 \times 10^8\,M^{-1}\,sec^{-1}$, in benzene.[11] However, DPBF is not soluble in water and was therefore modified with polar Me_2N, Me_3N^+, or CO_2H groups to obtain dyes **I**–**III** (Scheme 2 and the Experimental Section), which turned out to be soluble in water at pH 7 up to concentrations of at least 3 mM. Doubly positively charged dye **II** is not membrane permeable, whereas monocharged **I** and negatively charged **III** are permeable (Figure 2). The latter two compounds were not toxic to HL-60 cells at concentrations of up to 5 μM. By using flow cytometry, we tested whether dyes **I** and **III** are suitable for monitoring the formation of $^1O_2$ in live HL-60 cells. First, the cells were loaded with photosensitizer In**P**–OH (Supporting Information, Figure S26). $^1O_2$ was generated by exposure of the cells to red light (635 nm). Both dyes were shown to be stable in the cells in the absence of the photosensitizer. In its presence, they decomposed efficiently and, thereby indicated the formation of $^1O_2$. As expected, the rate of the decomposition reaction is proportional to the concentration of the photosensitizer (Figure 3; Supporting Information, Figure S27). Unfortunately, at high concentrations, dye **I** causes denaturation of ODN duplexes, for example, the deactivated catalyst (Figure 1), and thus triggers $^1O_2$ generation in the absence of a nucleic acid target. We suppose that this effect is due to unspecific interactions of the positively charged dye with the negatively charged nucleic acid duplexes. This is confirmed by the fact that negatively charged dye **III** does not affect the duplex stability. The latter compound was used in all further experiments for $^1O_2$ detection because of this favorable property.

Under physiological conditions and at low concentration (300 nM), the known **P**–ODN1 does not catalyze the photo-

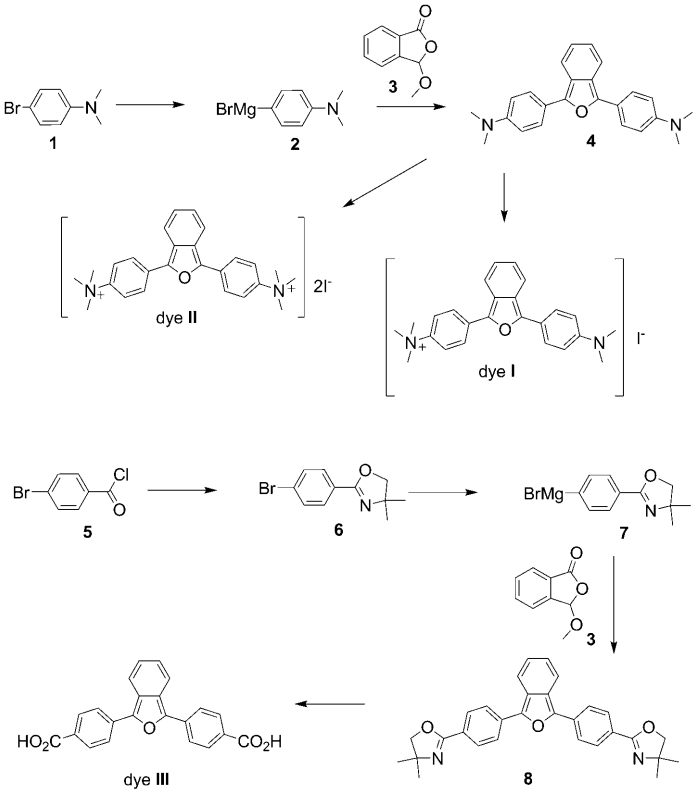

Scheme 2. Water-soluble derivatives (dyes **I**–**III**) of 1,3-diphenylisobenzofuran prepared for the detection of singlet oxygen ($^1O_2$) in live mammalian cells.

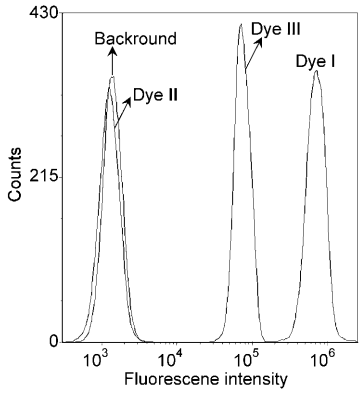

Figure 2. Monitoring uptake of fluorogenic $^1O_2$ scavengers (dyes **I**–**III**) in live HL-60 cells by using flow cytometry. The intensity of emission at 530 nm (excitation at 488 nm) is plotted versus the number of events (cells). The background trace is a negative control (no dye was added). Cells (10^6 cells mL^{-1}) were incubated in RPMI medium containing 10% fetal calf serum (FCS). Dyes were added at the final concentration of 5 μM. The measurements were conducted 10 min after addition of the dyes to the cell suspension. Fluorescence intensity is given in arbitrary units.

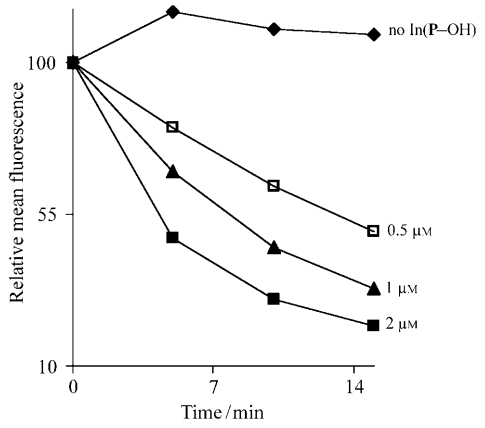

Figure 3. Monitoring of the generation of $^1O_2$ in live HL-60 cells by using dye **III** and flow cytometry. Cells (10^6 cells mL^{-1}) were first loaded with the corresponding amount of In**P**–OH (concentrations shown on the plot), washed twice with phosphate-buffered saline (PBS), and incubated with dye **III** (5 μM) in RPMI with 10% FCS for 10 min. The cells were then irradiated with red light (635 nm). The mean fluorescence of the cells that were not exposed to the light was taken as 100%.

decomposition of dye **III** in vitro, whereas its In^{3+} derivative, In**P**–ODN1, is an efficient catalyst of this reaction (Figure 4). The activity of the latter compound can be controlled by nucleic acids. In particular, In**P**–ODN1 forms a stable duplex with **Q**–ODN7, which is practically not fluorescent (Supporting Information, Figure S28). Complementary DNA12 (1 equiv) releases In**P**–ODN1 from the duplex; this release is manifested by an approximately 30-fold increase in the fluorescence intensity. The In**P**–ODN1 (300 nM) activated in this way speeds up the photodecomposition of 700-fold excess dye **III** by a factor of 6.1 relative to the background reaction (Figure 4). A turnover number (TON) of 377 is achieved at a constant turnover frequency (TOF) of $(10\pm1)\ min^{-1}$ within 40 min. After this time, the reaction slows down. A maximal TON of 512 is reached within 100 min. The reaction can be also controlled by RNA targets. In particular, RNA13, which has the same sequence as DNA12, produces a TON of 376 under similar conditions.

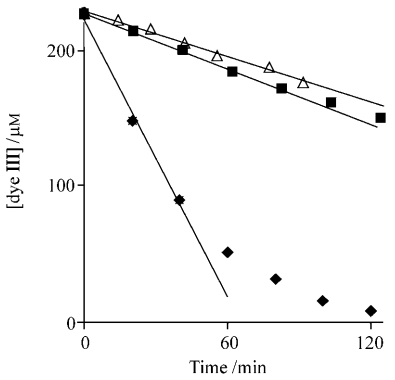

Figure 4. Decomposition of dye **III** (0.23 mM) upon illumination with red light ($\lambda=635$ nm, 2.59 mJ s^{-1}) under aerobic conditions in phosphate buffer (10 mM, pH 7, with 150 mM NaCl) in the presence of **P**–ODN1 (300 nM, ■) or In**P**–ODN1 (300 nM, ◆) or in the absence of any photosensitizer (background, △). Solid lines represent regions of constant rate of dye **III** decomposition. The experimental error of the determined concentrations of dye **III** was found to be less than 5%.

Next, we tested whether this assay can detect single mismatches in nucleic acids. The duplex In**P**–ODN1/**Q**–ODN7 was found to be insufficiently sequence specific: in the best case, the photodecomposition of dye **III** (0.23 mM) in the presence of mismatched DNA14 (T8→A8 mutation) is only 1.4 times slower than that in the presence of matched DNA12. To improve this property, we substituted duplex In**P**–ODN1/**Q**–ODN7 for a hairpin-structured conjugate In**P**–ODN2–**Q** (Scheme 1B). Such probes are known to be highly sequence specific.[12] As expected, In**P**–ODN2–**Q** is only weakly fluorescent in the folded state. Complementary DNA15 opens up the hairpin and restores its fluorescence, whereas mismatched DNA16 (G15→C15 mutation) has no effect (Figure 5). Correspondingly, the photodecomposition of dye **III** (0.23 mM) by In**P**–ODN2–**Q** (300 nM) in the presence of DNA16 is not distinguishable from that in the absence of any DNA. In contrast, the complementary DNA

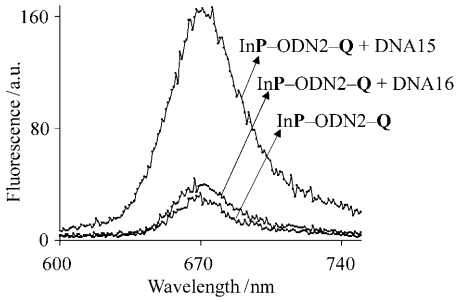

Figure 5. Fluorescence spectra (excitation at 635 nm) of InP–ODN2–Q (1 μM) under different conditions. Concentrations of DNA15 and DNA16: 5 μM. Buffer: 10 mM phosphate buffer, pH 7, with 150 mM NaCl. Fluorescence intensity is given in arbitrary units: a.u.

accelerates the decomposition of dye **III** by 6.5-fold with respect to the background reaction (Figure 6).

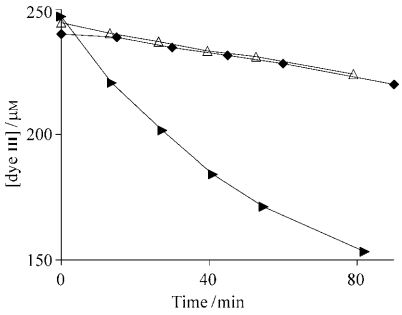

Figure 6. Decomposition of dye **III** (0.23 mM) upon illumination with red light ($\lambda=635$ nm, 2.59 mJ s^{-1}) under aerobic conditions in phosphate buffer (10 mM, pH 7, with 150 mM NaCl) in the presence of In**P**–ODN2–**Q** (300 nM) alone (◆) or with mismatched DNA16 (3 μM, △) or matched DNA15 (3 μM, ●). The experimental error of the determined concentrations of dye **III** was found to be less than 5%.

Furthermore, we explored the TON that this reaction is able to generate. Concentrations of the deactivated catalyst and DNA12 were kept constant at 300 nM while the concentration of dye **III** was increased. At the highest concentration of substrate tested (3 mM, 10^4 excess), a TON of 6373 could be achieved in 44.6 h. In 24 h, this reaction produces a TON of 4533, which represents an average TOF of 3.1 min^{-1}. The best DNA-dependent chemical reaction reported to date[13] generates a TON of 402 during the same time period, with a TOF of 0.28 min^{-1} (Table 1). Importantly, under these comparable conditions, our reaction has a signal-to-noise ratio (S/N) that is more than three times better: S/N = 7.2 rather than S/N = 2.[13] The dependence of the TON on the concentration of dye **III** is linear (Figure 7). No saturation is observed, even at the highest concentration of dye used. This indicates that the catalyst, In**P**, is not bleached even after the generation of over 6000 equivalents of $^1O_2$. Therefore, we expect that this photoreaction may produce even larger TONs at higher concentrations of dye **III**.

Table 1. Comparison of the reaction reported in this paper with the best nucleic acid dependent chemical reactions reported to date.

[Probes]/[Target]	Signal-to-noise ratio[a]	TOF [min^{-1}][b]	TON, time[c]	Reference
10^4	2	0.28	402, 24 h	[13]
10^3	7	0.15	215	[13]
10^4		0.16	226	[15]
10^2		13	50	[16]
10^4		0.03	40	[17]
10^4		0.06	92	[18]
50			7	[5a]
5		0.02	5	[2b]
10^4	7	3.4	4533, 24 h	this work
		2.4	6373, 44.6 h	this work

[a] Ratio of initial rates of chemical reactions in the presence and absence of a template nucleic acid. [b] TOF: turnover frequency. [c] TON: turnover number.

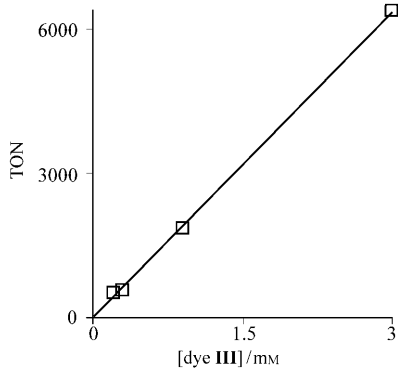

Figure 7. Dependence of the maximal turnover numbers (TON) in the photochemical decomposition of dye **III** in the presence of [In**P**–ODN1/**Q**–ODN7] (300 nM) and [DNA12] (300 nM) on the concentration of dye **III**. Samples were irradiated with red light ($\lambda = 635$ nm, 2.59 mJ s^{-1}). Buffer: 10 mM phosphate, pH 7, with 150 mM NaCl. The solid line corresponds to a linear fit of the experimental data shown as □.

Finally, we studied whether our duplexes could be activated in live cells by endogeneous RNAs. First, we prepared two pairs of deactivated catalysts containing 2′-OMe RNAs in place of ODNs. 2′-OMe RNAs are known to be significantly more resistant to intracellular nucleases than natural ODNs.[15] In each pair, one duplex (the scrambled probe) was designed to be inert, whereas the second one was supposed to bind 28S rRNA in the cell and produce the active photosensitizer (the 28S RNA probe). In the first pair, the duplexes consisted of a 16-mer In**P**–2′-OMe-RNA and a 22-mer **Q**-2′-OMe-RNA, whereas the strands were longer in the second pair: correspondingly, a 20-mer and a 30-mer. The shorter duplexes were shown to be unstable in the cell (Supporting Information, Figure S29). Therefore, all further experiments were conducted with the longer ones. The deactivated catalysts (In**P**–2′-OMe-RNA/**Q**-2′-OMe-RNA) were brought into HL-60 cells by using a pore-forming peptide, streptolysin O (SLO). The cells were then loaded with dye **III** and exposed to the red light. $^1O_2$ formation correlated with a decrease in the fluorescence intensity of dye **III**. This signal was quantified by the flow cytometry. We observed that the scrambled probe (In**P**–2′-OMe-RNA5/**Q**-2′-OMe-RNA10) does not generate $^1O_2$ upon exposure of the cell to red light for up to 25 min, which indicates that the duplex is stable in the cell within this time period (Figure 8). Under the same conditions, the positive control In**P**–2′-OMe-RNA produces large amounts of $^1O_2$. We were pleased to observe that the 28S rRNA probe (In**P**–2′-OMe-RNA6/**Q**-2′-OMe-RNA11) is activated in the cell, which is reflected in the time-dependent generation of $^1O_2$ (Figure 8). The scrambled probe (■ in Figure 8, bottom) starts producing $^1O_2$ 25 min after the beginning of the reaction. When we introduced a one-hour incubation period before starting the experiment,

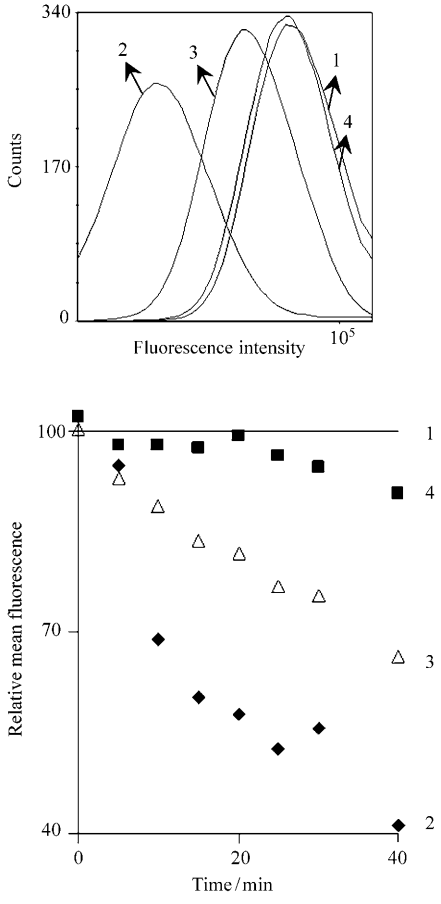

Figure 8. Monitoring of the formation of $^1O_2$ in live HL-60 cells by using flow cytometry. Concentration of dye **III**: 5 μM; concentration of each conjugate: 1 μM. Top) Intensity of emission at 530 nm (excitation at 488 nm) is plotted versus the number of events (counts = cell numbers): trace 1: negative control (no conjugates were added); trace 2: positive control (In**P**–2′-OMe-RNA5); trace 3: 28S rRNA probe (In**P**–2′-OMe-RNA6/**Q**–2′-OMe-RNA11); trace 4: scrambled probe (In**P**–2′-OMe-RNA5/**Q**–2′-OMe-RNA10). Cells were irradiated with red light (635 nm) for 25 min before the measurements. Bottom) The mean fluorescence of cells that were not incubated with any conjugates was taken as 100% (horizontal line). The trace numbering is the same as in (A).

the activities of the scrambled and 28S rRNA probes became indistinguishable from each other (Supporting Information, Figure S30). These facts indicate that the 2-OMe-RNA duplexes are not fully stable in the cell within the time period of the experiment, which is in agreement with reported data.[14] This limits the amplification potential of our assay. We hypothesize that the background process of duplex decomposition could be either slowed down or fully eliminated by the substitution of 2′-OMe-RNAs for more stable nucleic acid mimics, for example, peptide nucleic acids (PNAs) and hybrids of locked nucleic acids (LNAs) and 2′- OMe-RNAs. We are currently exploring these possibilities in our laboratories.

Conclusion

We have developed a nucleic acid dependent photosensitizer, which is functional under physiological conditions, is able to generate over 6000 equivalents of toxic singlet oxygen per equivalent of catalyst, and is highly sequence specific. We have demonstrated that the activity of this compound in live human cells is efficiently controlled by specific endogeneous ribonucleic acids. This is the first example of a live-cell-compatible gene-specific photosensitizer. Such agents may be used to obtain highly selective photodynamic drugs.

Experimental Section

Commercially available chemicals of the best quality from Aldrich/Sigma/Fluka (Germany) were obtained and used without purification. The reagents for DNA synthesis were obtained from Proligo Biochemie GmbH (Germany), Glen Research (USA), or Link Technologies (UK). HPLC-purified DNAs and RNAs were purchased from IBA GmbH (Germany). MALDI-TOF mass spectra were recorded on a Bruker BIFLEX III spectrometer. The matrix mixture (2:1 v/v) was prepared from 6-aza-2-thiothymine (ATT, saturated solution in acetonitrile) and diammonium citrate (0.1 M in water). Samples for mass spectrometry were prepared by the dried-droplet method by using a 1:2 probe/matrix ratio. Mass accuracy with external calibration was 0.1% of the peak mass, that is, ±6.0 at m/z 6000. Preparative and analytical HPLC was performed at 60°C on a Shimadzu liquid chromatograph equipped with a UV detector and a Macherey–Nagel Nucleosil C4 250×4.6 mm column. UV/Vis spectra were measured on a Varian Cary 100 Bio UV/Vis spectrophotometer by using 1 cm optical path black-wall absorption semi-microcuvettes (Hellma GmbH, Germany) with a sample volume of 0.7 mL. These cuvettes were also used for photochemical experiments. Light from a red laser (635 nm, 2.59 mW) was applied from the top of the cuvette by using an optical fiber. Fluorescence spectra were acquired on a Varian Cary Eclipse fluorescence spectrophotometer by using black-wall fluorescence semi-microcuvettes (Hellma GmbH, Germany) with a sample volume of 0.7 mL. The fluorescence of dyes **I**–**III** in live HK-60 cells was quantified by using an Accuri C6 Flow cytometer. The data were processed by using the CFLow Plus (Accuri) and FCS Express V3 (De Novo Software) software packages.

1,3-Di(4-dimethylaminophenyl)isobenzofuran (4; Scheme 2): A Grignard reagent (**2**) was first prepared from 4-bromo-*N*,*N*-dimethylaniline (1, 12 g, 60.0 mmol) and Mg turnings (1.46 g, 60.0 mmol) in tetrahydrofuran (THF; 40 mL) by using a standard protocol. The resulting solution was added dropwise to solution of methyl 2-formylbenzoate pseudoester[19] (**3**; 4.0 g, 24.4 mmol) in THF (30 mL) at 0°C under argon. The reaction mixture was slowly (2 h) heated up to 22°C and then stirred overnight at this temperature. The resulting suspension was cooled down to 0°C, and an aqueous solution of hydrochloric acid (15%, 15 mL) was added dropwise. The reaction mixture turned deep red. The cooling bath was removed, and the mixture was left to stir under argon for 1 h. The aqueous solution was washed with diethyl ether several times. It was then neutralized with Et_3N, and the product was extracted with diethyl ether. The combined diethyl ether extracts were dried over Na_2SO_4, the diethyl ether was evaporated, and the residue was purified by column chromatography by using a mixture of hexane and Et_2O (2:1). The yield of product **4** (yellow crystalline compound) was 2.5 g (29%); TLC (EtOAc/hexane 1:4): R_f=0.34; ^{1}H NMR (600 MHz, [D$_6$]acetone): δ=7.83 (m, 4H), 7.79 (m, 2H), 6.92 (m, 2H), 6.88 (m, 4H), 3.01 ppm (s, 12H); ESI-MS, positive mode: m/z calcd for $C_{24}H_{24}N_2O$ $[M]^{2+}$: 178.09; found: 178.09.

1-(4-Dimethylaminophenyl)-3-(4-trimethylaminoniumphenyl)isobenzofuran iodide (dye I): A mixture of compound **4** (178 mg, 0.5 mmol), K_2CO_3 (500 mg), and excess of MeI (1 mL) in acetone (10 mL) was stirred at 22°C for 24 h under argon. The insoluble material was filtered off and washed with acetone several times. The filtrate was collected, and the acetone was evaporated to yield dye **I** (200 mg, 81%) as red crystals: ^{1}H NMR (200 MHz, [D$_6$]dimethylsulfoxide (([D$_6$]DMSO)): δ=8.15–8.01 (m, 4H), 7.99–7.87 (m, 4H), 7.20–7.01 (m, 2H), 6.88 (d, 2H), 3.66 (s, 9H), 3.01 ppm (s, 6H); ESI-MS, positive mode: m/z calcd for $C_{25}H_{27}N_2O$ (the cationic part of dye **I**): 371.13; found: 371.20; UV/Vis (in PBS containing 10 mM phosphate and 150 mM NaCl, pH 7): λ=302, 437 nm; fluorescence spectrum (in PBS buffer as above): $\lambda_{excitation}$=437 nm; $\lambda_{emission}$=595 nm.

1,3-Di(4-trimethylaminoniumphenyl)isobenzofuran diiodide (dye II): A mixture of compound **4** (178 mg, 0.5 mmol), K_2CO_3 (500 mg), and an excess of MeI (1 mL) in *N*,*N*-dimethylformamide (DMF; 10 mL) was stirred at 22°C for 24 h under argon. The solvent was removed under 0.01 mbar pressure at 50°C, the residue was washed with methanol several times, and the filtrate was collected. The solvent was evaporated, and the residue was recrystallized from methanol to yield dye **II** (208 mg, 65%) as orange crystals: ^{1}H NMR (200 MHz, [D$_6$]DMSO): δ=8.31–8.26 (m, 4H), 8.14–8.09 (m, 6H), 7.29–7.24 (m, 2H), 3.70 ppm (s, 18H); ESI-MS, positive mode: m/z calcd for $C_{26}H_{30}N_2O$ (the dicationic part of dye **II**): 193.11; found: 193.05; UV/Vis (in PBS buffer as above): λ=274, 413 nm; fluorescence spectrum (in PBS buffer as above): $\lambda_{excitation}$=413 nm; $\lambda_{emission}$=453, 478 nm.

1,3-Di(4-(4,4-dimethyloxazolin-2-yl)phenyl)isobenzofuran (8): Grignard reagent **7** was prepared from 2-(4-bromophenyl)-4,4-dimethyl-2-oxazoline[20] (**6**; 5.1 g, 20.0 mmol) and Mg turnings (0.51 g, 21 mmol) in THF (20 mL).[21] After all of the Mg turnings had dissolved, the solution was added dropwise to a solution of methyl 2-formylbenzoate pseudoester (**3**) in THF (25 mL) at 0°C. The cooling bath was removed, and the mixture was left to stir overnight. The aqueous HCl solution (10%, 15 mL) was then added at 0°C, and stirring was continued for an additional hour. The water layer was washed several times with diethyl ether. (The product of the reaction stays in the aqueous phase.) The aqueous phase was carefully neutralized with sodium hydroxide solution, and the product was extracted with diethyl ether. The combined diethyl ether extracts were dried over Na_2SO_4, and the solvent was evaporated. Recrystallization of the residue from diethyl ether yields the analytically pure product (3.95 g, 85%): ^{1}H NMR (200 MHz, $CDCl_3$): δ=8.03 (m, 8H), 7.88 (m, 2H), 7.11 (m, 2H), 4.14 (s, 4H), 1.42 ppm (s, 12H); ESI-MS, positive mode: m/z calcd for $C_{30}H_{29}N_2O_3$ $[M+H^+]^+$: 465.21; found: 465.21.

1,3-Di(4-carboxyphenyl)isobenzofuran (dye III): A solution of compound **8** (1.0 g, 2.2 mmol) in aqueous HCl (3 M, 50 mL) was heated to reflux for 1 h. The precipitate formed was filtered, washed with water, and redissolved in 20% sodium hydroxide in methanol (prepared from a 50% solution of sodium hydroxide in water). The resulting solution was heated to reflux for another hour. The sodium hydroxide solution was then acidified with aqueous HCl (9 M) until pH 1 was reached; this resulted in precipitation of dye **III**. The precipitate was filtered, washed with water, and then dried at 0.01 mbar pressure. The yield of dye **III** was 0.51 g (65%): TLC (THF/CH_2Cl_2 1:9, with a drop of acetic acid): R_f=0.57; ^{1}H NMR

(200 MHz, [D$_6$]DMSO): δ = 13.06 (brs, 2H), 8.13 (m, 4H), 8.06 (m, 6H), 7.20 ppm (m, 2H); ESI-MS, negative mode: *m*/*z* calcd for $C_{22}H_{13}O_5$ [dye **III**−H$^+$]$^-$: 357.08; found: 357.07; UV/Vis (in PBS buffer as above): λ = 282, 430 nm; fluorescence spectrum (in PBS buffer as above): $\lambda_{excitation}$ = 430 nm; $\lambda_{emission}$ = 476, 502 nm.

Pheophytin a: Spirulina powder (500 g) was mixed with acetone (2 L) and liquid nitrogen (2 L) was slowly added while the mixture was stirred with a mechanical stirrer. The mixture was then allowed to melt, and the resulting slurry was heated to reflux for two hours and filtered through a Buchner funnel. The precipitate obtained was washed twice with acetone and discarded. Acetic acid (6 mL) was added to the filtrate and all volatile compounds were removed at 0.01 mbar pressure. The crude product was purified by column chromatography to give pheophytin a (**9**; yield: 5 g). Conditions for column chromatography: carotenoids (red, yellow bands) were eluted with 5% petroleum ether in CH_2Cl_2; a black band corresponding to the product was eluted with 20% ethyl acetate in CH_2Cl_2: TLC (CH_2Cl_2/EtOAc 15:1): R_f = 0.64; the ^{1}H and ^{13}C NMR spectra of the product were in agreement with literature data;[22] ESI-MS, positive mode: *m*/*z* calcd for $C_{55}H_{75}N_4O_5$ [*M*+H$^+$]$^+$: 871.57; found 871.48.

Pheophorbide a allyl ester: Pheophytin a (3 g, 3.44 mmol) and sulphuric acid (2 mL) were stirred in allyl alcohol (100 mL) at 22 °C for 48 h. The solution was diluted with water (200 mL), neutralized with aqueous saturated $NaHCO_3$, and extracted twice with dichloromethane. The combined organic extracts were dried over Na_2SO_4, the solvent was removed, and the residue was dried at 0.01 mbar pressure. The crude product was purified by column chromatography to yield pheophorbide a allyl ester (**10**; 1.4 g, 64%, black solid): TLC (CH_2Cl_2/EtOAc 15:1): R_f = 0.44; ^{1}H NMR: (400 MHz, $CDCl_3$): δ = 9.47 (s, 1H), 9.32 (s, 1H), 8.56 (s, 1H), 7.97–7.91 (m, 1H), 6.28–6.14 (m, 2H), 6.27 (s, 1H), 5.82–5.71 (m, 1H), 5.20–5.09 (m, 2H), 4.50 (m, 2H), 4.45 (m, 1H), 4.24 (m, 1H), 3.90 (s, 3H), 3.68 (s, 3H), 3.64 (m, 2H), 3.39 (s, 3H), 3.18 (s, 3H), 2.65 (m, 1H), 2.54 (m, 1H), 2.37 (m, 1H), 2.24 (m, 1H), 1.83 (m, 3H), 1.69–1.65 (m, 3H), 0.52 (s, 1H, NH), −1,66 ppm (s, 1H, NH); ^{13}C NMR ($CDCl_3$): δ = 189.60, 172.53, 172.14, 169.59, 161.11, 155.59, 150.93, 149.62, 145.16, 142.01, 137.90, 136.45, 136.22, 131.90, 131.81, 129.03, 128.95, 122.74, 118.38, 105.19, 104.38, 97.49, 93.08, 77.20, 65.21, 64.69, 52.84, 51.08, 50.09, 31.08, 29.75, 23.07, 19.39, 17.38, 12.09, 12.07, 11.17 ppm; high-resolution ESI-MS, positive mode: *m*/*z* calcd for $C_{38}H_{41}N_4O_5$ [*M*+H$^+$]$^+$: 633.3071; found: 633.3096.

Pyropheophorbide a allyl ester: Pheophorbide a allyl ester (1.4 g, 2.21 mmol) was dissolved in 2,4,6-collidine (70 mL) and stirred for 5 h at 170 °C under an argon atmosphere. After this, the solvent was evaporated at 0.01 mbar pressure, and the crude product was purified by column chromatography to yield the product (902 mg, 71%) as a black solid: TLC (CH_2Cl_2/EtOAc 15:1): R_f = 0.30; ^{1}H NMR: (400 MHz, $CDCl_3$): δ = 9.40 (s, 1H), 9.30 (s, 1H), 8.55 (s, 1H), 7.99–7.92 (m, 1H), 6.28–6.13 (m, 2H), 5.88–5.78 (m, 1H), 5.29–5.09 (m, 2H), 5.26–5.15 (m, 2H), 4.54 (m, 2H), 4.50 (m, 1H), 4.31 (m, 1H), 3.63 (s, 3H), 3.60 (m, 2H), 3.40 (s, 3H), 3.17 (s, 3H), 2.72 (m, 1H), 2.59 (m, 1H), 2.33 (m, 2H), 1.83 (m, 3H), 1.68–1.65 (m, 3H), 0.38 (s, 1H, NH), −1.76 ppm (s, 1H, NH); ^{13}C NMR ($CDCl_3$): δ = 196.16, 172.68, 171.29, 160.18, 155.08, 150.65, 148.92, 144.87, 141.46, 137.76, 136.08, 135.96, 135.72, 131.90, 131.47, 129.15, 128.22, 122.45, 118.55, 105.97, 103.96, 97.08, 92.95, 77.20, 65.25, 51.60, 49.92, 48.03, 31.02, 29.79, 23.13, 19.38, 17.40, 12.08, 12.00, 11.16 ppm; high-resolution ESI-MS, positive mode: *m*/*z* calcd for $C_{36}H_{39}N_4O_3$ [*M*+H$^+$]$^+$: 575.3017; found: 575.3000.

In(pyropheophorbide a allyl ester)Cl: Pyropheophorbide a allyl ester (226 mg, 0,393 mmol), $InCl_3$ (1.356 g, 6.13 mmol), NaOAc (2.26 g, 27.6 mmol), and K_2CO_3 (2.26 g, 16.4 mmol) in benzene (68 mL) were heated to reflux for 18 h under an argon atmosphere. The suspension was then neutralized with acetic acid and extracted with several portions of water. The combined aqueous phases were extracted with CH_2Cl_2. The combined organic phases were dried over Na_2SO_4, and the solvent was evaporated in vacuo. The crude product was purified by column chromatography to give the product (175 mg, 62%) as a black solid: TLC (CH_2Cl_2/EtOAc 15:1): R_f = 0.36; ^{1}H NMR: (200 MHz, $CDCl_3$): δ = 9.69 (s, 1H), 9.49 (s, 1H), 8.53 (s, 1H), 7.98–7.91 (m, 1H), 6.27–6.13 (m, 2H), 5.95–5.85 (m, 1H), 5.33–4.96 (m, 2H), 5.32–5.08 (m, 2H), 4.62 (m, 2H), 4.56 (m, 1H), 4.32 (m, 1H), 3.82–3.75 (m, 2H), 3.65 (s, 3H), 3.35 (s, 3H), 3.30 (s, 3H), 2.86–2.68 (m, 1H), 2.61 (m, 1H), 2.50 (m, 1H), 2.24–2.10 (m, 1H), 2.02 (m, 3H), 1.74–1.68 ppm (m, 3H); ^{13}C NMR ($CDCl_3$): δ = 195.24, 172.59, 168.94, 160.68, 155.89, 153.72, 150.51, 146.43, 146,22, 145.31, 144.44, 140.40, 136.62, 135.48, 134.80, 131.95, 129.20, 122.67, 118.62, 107.77, 105.70, 100.32, 92.38, 77.20, 65.38, 50.83, 49.59, 48.11, 30.22, 29.69, 23.21, 19.58, 17.29, 12.73, 12.21, 11.03 ppm; high-resolution ESI-MS, positive mode: *m*/*z* calcd for $C_{36}H_{36}N_4O_3In$ [*M*−Cl$^-$]$^+$: 687.1821; found: 687.1813.

In(pyropheophorbide a)Cl (In(P−OH): [Pd(PPh$_3$)$_4$] (7.2 mg, 6.21 μmol) and PPh_3 (1.1 mg, 4.13 μmol) in CH_2Cl_2 (1 mL) were added to suspension containing In(pyropheophorbide a allyl ester)Cl (20 mg, 27.67 μmol) and (NH_2Et_2)(HCO_3) (20.9 mg, 160 μmol) in CH_2Cl_2 (5 mL). The reaction was completed in 15 min, according to TLC analysis. The resultant solution was directly loaded onto a chromatography column. In(**P**-OH) (17 mg, 90.2%) was eluted with 5% methanol in CH_2Cl_2 (with a few drops of acetic acid): TLC (CH_2Cl_2/MeOH 50:1): R_f = 0.25; ^{1}H NMR: (400 MHz, $CDCl_3$): δ = 9.68 (s, 1H), 9.45 (s, 1H), 8.26 (s, 1H), 7.97–7.90 (m, 1H), 6.23–6.07 (m, 2H), 4.76 (m, 1H), 4.60 (m, 1H), 3.94–3.72 (m, 3H), 3.64 (s, 3H), 3.53 (s, 1H) 3.29 (s, 3H), 3.28 (s, 3H), 1.74–1.71(m, 3H), 1.50–1.00 (m, 4H), 1.30 ppm (m, 3H); ^{13}C NMR ($CDCl_3$): δ = 195.54, 173.02, 168.67, 160.69, 155.89, 153.62, 150.55, 146.58, 146.34, 144.83, 144.50, 139.72, 135.97, 134.29, 132.55, 129.46, 122.03, 107.53, 105.42, 99.78, 92.45, 77.20, 50.59, 47.88, 47.34, 30.56, 28.56, 22.34, 19.61, 17.25, 12.78, 12.28, 11.10 ppm; high-resolution ESI-MS, positive mode: *m*/*z* calcd for $C_{33}H_{32}InN_4O_3$ [*M*−Cl$^-$]$^+$: 647.1508; found: 647.1501. This complex was prepared before by a different method.[8]

Synthesis of conjugates of photosensitizers with either ODNs or 2′-OMe-RNAs: Solid-support-bound 5′-amino-modified ODNs (MMT-HN–ODNs; MMT: mono(4-methoxyphenyl)diphenyl) and their 2-OMe-RNA analogues (MMT-HN–2′-OMe-RNAs) were prepared on an Expedite 8909 PNA/DNA synthesizer by using standard DNA or 2′-OMe-RNA phosphoramidites (A and C: benzyl protected; G: dmf protected), standard solid supports (controlled pore glass (CPG)) with the first nucleotide attached), and 5′-MMT-amino-modifier phosphoramidites from Links Technologies (UK). 5′-MMT-HN–ODN2–BHQ-3 was prepared analogously by using 3′-BHQ-3 CPG (Glen Research, USA) in place of the standard CPG solid support. The MMT group was then cleaved by treatment of the CPG-bound conjugates (1 μmol scale synthesis) with 1% trifluoroacetic acid (TFA) in CH_2Cl_2 (1 mL) for 3 min, washing of the samples with 1% TFA in CH_2Cl_2 (2×2 mL) and CH_2Cl_2 (3×2 mL), and drying at 0.01 mbar pressure for 1 h. Finally, the photosensitizers were coupled under standard conditions. Typical protocols for these synthetic steps are given below.

Coupling of photosensitizers to nucleic acids and their mimics: The carboxylic acid (**P**−OH or In**P**−OH, 100 μmol), *O*-(benzotriazol-1-yl)-*N*,*N*,*N*′,*N*′-tetramethyluronium hexafluorophosphate (HBTU; 34 mg, 90 μmol), and 1-hydroxy-1*H*-benzotriazole (HOBT; 14 mg, 100 μmol) were dissolved in DMF (1 mL), and *N*,*N*-diisopropylethylamine (DIEA; 38 μL, 220 μmol) was added. This solution was vortexed and immediately added to the CPG-bound nucleic acid strand. The slurry obtained was left for 1 h with vigorous stirring. The CPG was filtered, washed with DMF (2×1 mL) and CH_3CN (2×1 mL), and dried under vacuum (10^{-2} mbar). The conjugates were deprotected and cleaved from the solid support with 27% aqueous ammonia solution at 22 °C for 24 h, followed by removal of excess ammonia with a stream of nitrogen, removal of the solid support by filtration, lyophilization of the filtrate, dissolution of the residue in water, and HPLC purification.

Determination of conjugate concentration by UV spectroscopy: HPLC-purified conjugates were lyophilized and dissolved in water (250 μL). Small samples from these solutions were diluted 250-fold with water, and their absorbances at 260 nm were measured. These values were used for calculation of the concentrations of the conjugates. Extinction coefficients of the conjugates were calculated as the sum of the extinction coefficients of the corresponding natural nucleotides and photosensitizers. The extinction coefficient of the previously uncharacterized In**P**−OH was determined to be 12000 $M^{-1}cm^{-1}$ at 260 nm.

Conditions of the HPLC purification of the conjugates: For the majority of the conjugates, the following gradient was used (solvent B: 1% H_2O in MeOH; solvent A: 0.1 M triethylammonium acetate buffer, pH 7): 5 min at 0% B, 0→90% B in 25 min, 10 min at 90% B. For In**P**–ODN2–Q, the following gradient was used (solvents as above): 5 min at 0% B, 0→90% B in 20 min, 10 min at 90% B. For **P**–ODN1, the following gradient was used (solvent B: CH_3CN; solvent A: 0.1 M triethylammonium acetate buffer, pH 7): 0→70% B in 35 min, 10 min at 90% B.

P–ODN1: Yield = 37%; HPLC: R_t = 27.5 min; MALDI-TOF MS: *m*/*z* calcd for $C_{183}H_{229}N_{59}O_{91}P_{15}$ $[M-H]^-$: 5173.20; found: 5173.20.

InP–ODN1: Yield = 36%; HPLC: R_t = 25.9 min; MALDI-TOF MS: *m*/*z* calcd for $C_{183}H_{226}N_{59}O_{91}P_{15}In$ $[M-2H^+]^-$: 5285.00; found: 5285.40.

InP–ODN2–Q: Yield = 21%; HPLC: R_t = 20.4 min; MALDI-TOF MS: *m*/*z* calcd for $C_{332}H_{405}N_{116}O_{165}P_{28}InNa$ $[M+Na^+-3H^+]^-$: 9660.92; found: 9663.02.

InP–2′-OMe-RNA3: Yield = 14%; HPLC: R_t = 27.0 min; MALDI-TOF MS: *m*/*z* calcd for $C_{207}H_{261}N_{63}O_{117}P_{16}In$ $[M-2H^+]^-$: 6113.71; found: 6102.44.

InP–2′-OMe-RNA4: Yield = 11%; HPLC: R_t = 26.8 min; MALDI-TOF MS: *m*/*z* calcd for $C_{208}H_{262}N_{66}O_{117}P_{16}In$ $[M-2H^+]^-$: 6168.81; found: 6151.45.

InP–2′-OMe-RNA5: Yield = 14%; HPLC: R_t = 26.7 min; MALDI-TOF MS: *m*/*z* calcd for $C_{248}H_{316}N_{76}O_{145}P_{20}In$ $[M-2H^+]^-$: 7415.61; found: 7414.55.

InP–2′-OMe-RNA6: Yield = 14%; HPLC: R_t = 26.4 min; MALDI-TOF MS: *m*/*z* calcd for $C_{250}H_{317}N_{81}O_{145}P_{20}In$ $[M-2H^+]^-$: 7510.61; found: 7502.38.

Cellular experiments: Streptolysin O (SLO) was used to reversibly permeabilize HL-60 cells in the suspension according to a previously reported protocol.[23] In particular, SLO (1000 U mL^{-1}) was activated in PBS containing 5 mM dithiothreitol and 0.05% bovine serum albumin (BSA) for 2 h at 37 °C. HL-60 cells (1×10^6 cells mL^{-1}) were washed twice with PBS, resuspended in the serum-free medium (100 μL), permeabilized by the addition of an optimized amount of SLO (10–15 U for 10^6 cells) and variable concentrations of conjugates, and then incubated at 37 °C for 10 min. The cellular membrane was sealed by the addition of RPMI-1640 medium (300 μL) with 10% FCS and further incubation at 37 °C for 20–30 min. The processes of permeabilization and sealing were monitored by flow cytometry. After the sealing, the cells were washed with PBS and resuspended in the medium (300 μL) with 10% FCS containing 5 μM of a singlet-oxygen scavenger (dye **I** or dye **III**). The cells were irradiated with the red light for definite periods of time.

Acknowledgements

We thank the German Research Council (Emmy-Noether Program, grant no. MO 1418/1-2 for A.M.), the Danish National Research Foundation, and the Ruprecht-Karls-Universität Heidelberg for funding this work.

[1] Recent reviews on nucleic acid directed reactions: a) A. P. Silverman, E. T. Kool, *Chem. Rev.* **2006**, *106*, 3775–3789; b) M. F. Jacobsen, E. Cló, A. Mokhir, K. V. Gothelf, *ChemMedChem* **2007**, *2*, 793–799; c) T. N. Grossmann, A. Strohbach, O. Seitz, *ChemBioChem* **2008**, *9*, 2185–2192.

[2] Papers on metal-complex-catalyzed chemical nucleic acid directed reactions: a) I. Boll, E. Jentzsch, R. Kraemer, A. Mokhir, *Chem. Commun.* **2006**, 3447–3449; b) I. Boll, R. Kraemer, J. Brunner, A. Mokhir, *J. Am. Chem. Soc.* **2005**, *127*, 7849–7856; c) J. Brunner, A. Mokhir, R. Kraemer, *J. Am. Chem. Soc.* **2003**, *125*, 12410–12411; d) F. H. Zelder, J. Brunner, R. Kraemer, *Chem. Commun.* **2004**, 902–903; e) N. Graf, M. Göritz, R. Krämer, *Angew. Chem.* **2006**, *118*, 4117–4119; *Angew. Chem. Int. Ed*, **2006**, *45*, 4013–4015; f) M. Nielsen, A. H. Thomsen, F. Kirpekar, K. V. Gothelf, *J. Org. Chem.* **2004**, *69*, 2240–2250; g) J. L. Czlapinski, T. L. Sheppard, *J. Am. Chem. Soc.* **2001**, *123*, 8618–8619; h) J. L. Czlapinsky, T. L. Sheppard, *ChemBioChem* **2004**, *5*, 127–129; i) C. S. Andersen, H. Yan, K. V. Gothelf, *Angew. Chem.* **2008**, *120*, 5651–5654; *Angew. Chem. Int. Ed.* **2008**, *47*, 5569–5572.

[3] Recent papers on organic nucleic acid directed reactions: a) J. M. Heemstra, D. R. Liu, *J. Am. Chem. Soc.* **2009**, *131*, 11347–11349; b) T. N. Grossmann, O. Seitz, *Chem. Eur. J.* **2009**, *15*, 6723–6730; c) R. M. Franzini, E. T. Kool, *ChemBioChem* **2008**, *9*, 2981–2988. Recent papers on applications of template reactions in the discovery of new drugs: d) B. N. Tse, T. M. Snyder, Y. Shen, D. R. Liu, *J. Am. Chem. Soc.* **2008**, *130*, 15611–15626 and references therein; e) M. H. Hansen, P. Blakskjær, L. K. Petersen, T. H. Hansen, J. W. Højfeldt, K. V. Gothelf, N. J. V. Hansen, *J. Am. Chem. Soc.* **2009**, *131*, 1322–1327.

[4] a) S. Sando, H. Abe, E. T. Kool, *J. Am. Chem. Soc.* **2006**, *128*, 263–268; b) H. Abe, E. T. Kool, *Proc. Natl. Acad. Sci. USA* **2006**, *103*, 263–268.

[5] a) Z. Pianowski, K. Gorska, L. Oswald, C. A. Merten, N. Winssinger, *J. Am. Chem. Soc.* **2009**, *131*, 6492–6497; b) K. Furukawa, H. Abe, K. Hibino, Y. Sako, S. Tsuneda, Y. Ito, *Bioconjugate Chem.* **2009**, *20*, 1029–1036; c) R. M. Franzini, E. T. Kool, *J. Am. Chem. Soc.* **2009**, DOI: 10.1021/ja904138v.

[6] Ruthenium catalyst active in live cells: a) C. Streu, E. Meggers, *Angew. Chem.* **2006**, *118*, 5773–5776; *Angew. Chem. Int. Ed.* **2006**, *45*, 5645–5648. Staudinger reaction with one of the substrates attached to the surface of live cells: b) E. Saxon, C. R. Bertozzi, *Science* **2000**, *287*, 2007–2010; c) M. J. Hangauer, C. R. Bertozzi, *Angew. Chem.* **2008**, *120*, 2428–2431; *Angew. Chem. Int. Ed.* **2008**, *47*, 2394–2397, and references therein.

[7] a) A. Okamoto, K. Tanabe, T. Inasaki, I. Saito, *Angew. Chem.* **2003**, *115*, 2606–2608; *Angew. Chem. Int. Ed.* **2003**, *42*, 2502–2504; b) K. Tanabe, H. Nakata, S. Mukai, S.-I. Nishimoto, *Org. Biomol. Chem.* **2005**, *3*, 3893–3897; c) E. Cló, J. W. Snyder, N. V. Voigt, P. R. Ogilby, K. V. Gothelf, *J. Am. Chem. Soc.* **2006**, *128*, 4200–4201.

[8] Y. Chen, X. Zheng, M. P. Dobhal, A. Gryshuk, J. Morgan, T. J. Dougherty, A. Oseroff, R. K. Pandey, *J. Med. Chem.* **2005**, *48*, 3692–3695.

[9] X. Ragàs, A. Jimènez-Banzo, D. Sànchez-Garcìa, X. Batllori, S. Nonell, *Chem. Commun.* **2009**, 2920, and references therein.

[10] C. Schweitzer, R. Schmidt, *Chem. Rev.* **2003**, *103*, 1685–1758.

[11] B. Stevens, S. R. Perez, J. A. Ors, *J. Am. Chem. Soc.* **1974**, *96*, 6846–6850.

[12] S. Tyagi, D. P. Bratu, F. R. Kramer, *Nat. Biotechnol.* **1998**, *16*, 49–53.

[13] T. N. Grossmann, O. Seitz, *J. Am. Chem. Soc.* **2006**, *128*, 15596–15597.

[14] J. F. Milligan, M. D. Matteucci, J. C. Martin, *J. Med. Chem.* **1993**, *36*, 1923–1937.

[15] C. Dose, S. Ficht, O. Seitz, *Angew. Chem.* **2006**, *118*, 5495–5499; *Angew. Chem. Int. Ed.* **2006**, *45*, 5369–5373.

[16] Z.-Y. J. Zhan, D. G. Lynn, *J. Am. Chem. Soc.* **1997**, *119*, 12420–12421.

[17] Y. Xu, N. B. Karalkar, E. T. Kool, *Nat. Biotechnol.* **2001**, *19*, 148–152.

[18] H. Abe, E. T. Kool, *J. Am. Chem. Soc.* **2004**, *126*, 13980–13986.

[19] T. M. Cresp, R. G. F. Giles, M. V. Sargent, C. Brown, D. O'N. Smith, *J. Chem. Soc. Perkin Trans. 1* **1974**, 2435–2447.

[20] A. I. Meyers, D. L. Temple, D. Haidukewych, E. D. Mihelich, *J. Org. Chem.* **1974**, *39*, 2787–2793.

[21] J. Einhorn, *Synlett* **2006**, 2035–2038.

[22] K. M. Smith, D. A. Goff, D. J. Simpson, *J. Am. Chem. Soc.* **1985**, *107*, 4946–4954.

[23] R. V. Giles, J. Grzybowski, D. G. Spiller, D. M. Tidd, *Nucleosides Nucleotides* **1997**, *16*, 1155–1163.

Received: August 27, 2009
Published online: November 5, 2009

